
Impact of bulk and nano zinc oxide on histopathology of *Labeo rohita*

Keerthika, V. and Rajan, M. R.*

Department of Biology, The Gandhigram Rural Institute-Deemed to be University Gandhigram-624302, Tamil Nadu, India.

Keerthika, V. and Rajan, M. R. (2023). Impact of bulk and nano zinc oxide on histopathology of *Labeo rohita*. International Journal of Agricultural Technology 19(2):487-504.

Abstract The UV-VIS analysis of bulk and nano zinc oxide was observed at 322 nm and 335nm. FT-IR spectral band was perceived at 401.12 cm^{-1} and 402 cm^{-1} . XRD reveals that both bulk and nano ZnO were crystalline hexagonal wurtzite in structure. The average was 65nm and 24nm. SEM photos revealed that chemically produced nano ZnO was spherical and evenly dispersed, in contrast to bulk zinc oxide which was rod-shaped. The purity of the particles is confirmed by the EDAX spectrum, which showed only Zn and O compound peaks for both bulk and chemically produced ZnO. The histological lesions such as basal hyperplasia, necrotic lamellae, a fusion of primary and secondary lamellae in the gill, melanomacrophages, pancreatic tissue, vacuolation, hepatic necrosis, apoptosis, oedema in the liver, Bowman's capsule extension and tubular distortion, glomerular enlargement and hemosiderin was detected in *Labeo rohita* kidney treated with bulk as well as nano zinc oxide when compared to the control.

Keywords: Histopathology, Gill, Liver, Kidney, Fish

Introduction

Nanoparticles are applied in many economic sectors including consumer products, the metal industry, transportation, cosmetics, pharmaceuticals, antimicrobial agents and agriculture (Jovanović and Palić, 2012). Due to their role as a transporter of nutrients, enzymes, and food additives and enhance the physical, chemical, and nutritional quality of feed, which has a major impact on the manufacturing of consumer products against microbial impacts (Can *et al.*, 2011). Metal oxide nanoparticles are produced and used on a large scale, which results in an unregulated environmental release. Nanoparticles are more attractive materials for manipulating, sensing, and detecting biological structures and systems than bulk particles. An increase in their relative surface area and quantum effects, which have an impact on their physical and chemical properties, are the main features that distinguish nanomaterials from their bulk counterparts (Nel *et al.*, 2006).

Amidst several metal oxide nanoparticles, zinc oxide plays a leading part in nanotechnology by virtue of its selectivity in contrast to other metal

* **Corresponding Author:** Rajan, M. R.; **E. mail:** mrrrajanbio@gmail.com

oxide micro and nanoparticles. Wide generation and immense use of zinc oxide affect the water entity. ZnO is one of the most pollutants present in water bodies, due to its effect on water-dwelling animals (Kahru and Dubourguier, 2010). Fish are considered indicators of ZnO contaminants in the water bodies because they live in the aqueous medium and are a significant source of food (Agah *et al.*, 2009). Fish is used as a model organism for monitoring the toxicity of the surroundings and ultimately affects normal growth. In polluted surroundings, the gills of fish are affected as the main site by the toxins. The kidney and liver are crucial detoxifying organs as well as primary organs for pollutant aggregation, bio-augmentation and evacuation (Murali *et al.*, 2017). Nanoparticles' hazardous effects depend on how they are exposed, for how long, and on their physical and chemical characteristics, such as size, shape, reactivity, and material composition (Lennart Treuel, 2013; Khan *et al.*, 2019). Analyzing the effect of metal oxide nanoparticles in fish by histopathological examinations of the specific target organ is an efficient way (Abdel-Warith *et al.*, 2011). Recent work has been reported for the nascent on the influence of nano and bulk zinc oxide on the histopathology of *Labeo rohita*.

Materials and methods

For the manufacture of zinc oxide nanoparticles, 0.5M of zinc acetate and 1 M of sodium hydroxide were prepared. Rapid mixing was carried out by putting 1M NaOH dropwise into the 0.5M of zinc acetate solution. The action pursued up to the emergence of eggshell precipitate and the pH stood from neutral to alkaline. After being cleansed with distilled water and ethanol to get rid of the byproducts, the solution was spun in a centrifuge at 3000 rpm for 10 min. The bottom layer was dried and calcined in a muffle furnace at 300 °C for 3 h. Ultimately, nano ZnO was shaped into powder using the pestle.

The manufactured nanoparticles were described by UV-Vis Spectrophotometer (JASCO-V-530), Fourier Transform Infrared Spectroscopy FTIR (JASCO FTIR-6200) X-Ray Diffraction (SHIMADZU Model XRD-6000), Scanning Electron Microscope (SEM)(LEO 1455 VP), and Energy Dispersive X-ray detection instrument (EDAX)(HORIBA 8121-H).

Healthy *Labeo rohita* fingerlings (5 ± 1 cm) were acquired from Palani, Tamil Nadu, India for the current study, and fish spent around 15 days getting used to the lab environment before the experiment ever started. In order to maintain the experimental animals' metabolic states more or less constant, fish were denied food for a full day prior to the experiment's start. Under static conditions, the acute toxicity test was carried out in accordance with the guidelines of the Organization for Economic Cooperation and

Development guideline (OECD, No.203, 1992). Five different bulk and nano ZnO concentrations were selected for median lethal concentration (LC₅₀) viz., 0, 3, 6, 12 and 24 mg/L and 0, 2, 4, 8 and 16 mg/L and 0 served as control. The identical circumstances were applied to each treatment, which was performed in triplicate. Groups of seven *Labeo rohita* were subjected to a range of bulk and nano ZnO concentrations over 96 hours. Mortalities were calculated at 24, 48, 72, and 96 hours, and dead fish were removed right away to prevent potential water quality degradation. For Probit Analysis, the LC₅₀ values were computed using SPSS software version 20.

Based on the acute toxicity test, 1/100th (T₁), 1/50th (T₂) and 1/10th (T₃) of LC₅₀ value were selected for the sub-acute toxicity test. The stock suspension was prepared the same as that of the acute toxicity test and fish were exposed for 14 days. This experiment was done in triplicate. For this investigation, a total of 60 fish were used. Under the same circumstances, a control (T₀) test without test suspension was performed. The fish were randomly selected in each concentration at the end of the seventh and fourteenth days of exposure, along with a control group, for histopathological investigation.

Results

The primary characterization of bulk and chemically synthesized nano zinc oxide particles using UV-Vis Spectrophotometer were analyzed between 300-500nm wavelengths. The high peak of absorbance was observed at 322nm for bulk zinc oxide and 335 nm for chemically synthesized ZnO NPs and presented in Figure 1a and 1b respectively. The 4000 - 400 cm⁻¹ region of the FTIR spectrum of bulk and nanoscale zinc oxide was examined. The FTIR spectral band of the bulk particles was presented in Fig. 2a and observed peaks are 3660.23, 3450.99, 3021.9, 2960.19, 2649.71, 2111.67, 1987.28, 1741.40, 1365.35 and 401.12 cm⁻¹ associated to alcohols O-H stretch, O-H stretching broad absorption hydroxyl, alkenes: C-H stretch, alkenes: C-H stretch, hydrocarbons: C-H stretch, C-C stretching vibration, C-H vibration, C=O stretch, CH bond and Zn- O stretching vibration. FTIR Spectrum of chemically synthesized nano zinc oxide (Figure 2b) shows bands at 3459.6 cm⁻¹ are associated with O-H stretching vibration, 2962.1 cm⁻¹ due to CH₃ and CH₂ stretching vibration, 1445.3 cm⁻¹ corresponds to C=O Stretching vibration, 902.5 cm⁻¹ observed CH₂ deformed vibration and 402 cm⁻¹ associated with broad Zn-O stretching vibration. The crystalline structure and crystal size of both bulk and chemically synthesized nano zinc oxide particles are analyzed by using XRD analysis. The XRD diffraction peaks of bulk ZnO particles are indexed as 31.687 °; 34.339 °; 36.172 °; 47.453 °; 56.507 °; 62.768 °; 66.281 °; 67.856 °; 68.981 ° and 76.908 ° which corresponds to planes 100, 002, 101,

102, 110, 103, 200, 112, 201 and 202 crystal plane respectively (Figure 3a). Chemically synthesized ZnO NPs are indexed as 31.371 °(100), 34.014 °(002), 47.161 °(102), 56.223 °(110), 62.492 °(103), 66.003 °(200), 67.593 °(112), 72.210 °(004) and 78.833 °(400) and are presented in Figure 3b. According to the hexagon form and wurtzite structure of ZnO described in JCPDS card no. 36-1451 all diffraction peaks of both bulk and ZnO NPs are indexed. Except for ZnO, there are no peaks that are typical of impurity phases, indicating that the samples are well-crystalline. Instead, sharp, narrow, strong peaks are detected. The average crystalline size of bulk and ZnO NPs was 65nm and 24nm calculated by the Scherrer formula. The morphology of bulk and chemically synthesized nano zinc oxide were analyzed by Scanning Electron Microscope and are presented in Figures 4a & 4b. SEM image shows that the bulk particles are rod-shaped and nano zinc oxide is spherical which is uniform in size and equally distributed. The elemental composition and purity of bulk and ZnO NPs analyzed by EDX are presented in Figures 5a & 5b. The EDX spectrum of bulk particles is recorded between 0 to 10KeV. The two highest peaks are directly from Zn at 1KeV and 8.5KeV, and one small peak at 0.5KeV is directly from O.

The normal gill structure in the control group is shown in Figure 6a, b, which documents histopathological changes in the Gill of *Labeo rohita* exposed to bulk zinc oxide. Gill subjected to bulk ZnO exhibits pathological diversity at the end of day seven, including lamellar aneurysm and rolling at the tips of secondary lamellae at T₁ (Figure 6c), as well as the beginning of basal hyperplasia, necrosis and chloride cell proliferation at T₂ (Figure 6e) and fusion of primary and secondary lamellae and mucus cells were observed at T₃ (Figure 6g) whereas, a fusion of primary and secondary lamellae, haemorrhage in primary lamellae at T₁ (Figure 7c), total fusion of gill lamellae and epithelial fusion at T₂ (Figure 7e) and oedema, curved tips of secondary lamellae fused and necrotic lamellae at T₃ (Figure 7g) exposed to nano ZnO. After the 14th day, the results of gill exposed to both bulk (Figure 6d,f, h) and nano zinc oxide (Figure 7d, f, h) revealed that complete fusion of primary and secondary lamellae, capillary and secondary lamellae dilution, haemorrhage, shorting of secondary lamellae and the aneurysm is appeared compared to that of control fish.

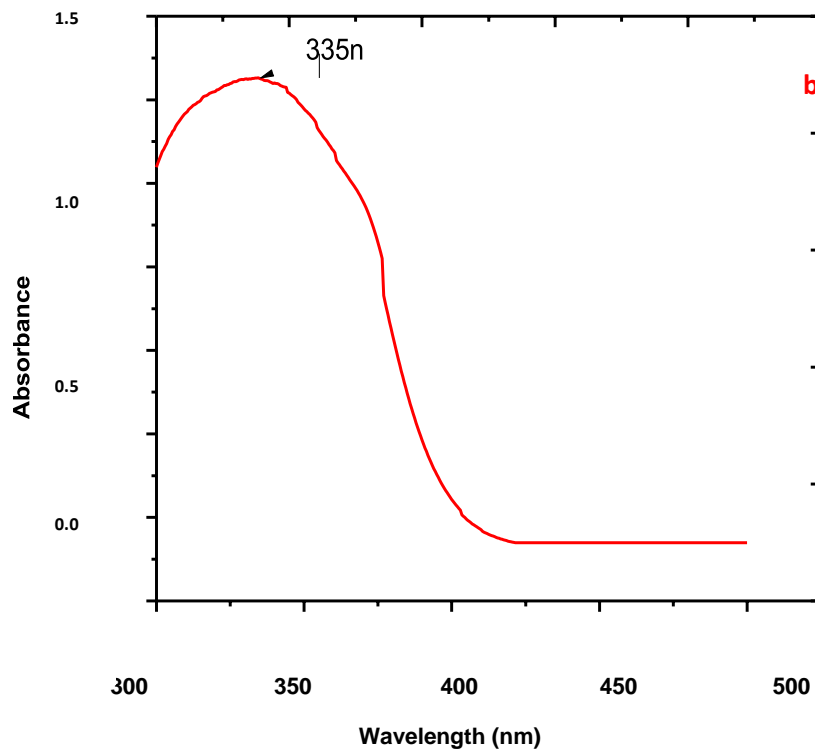
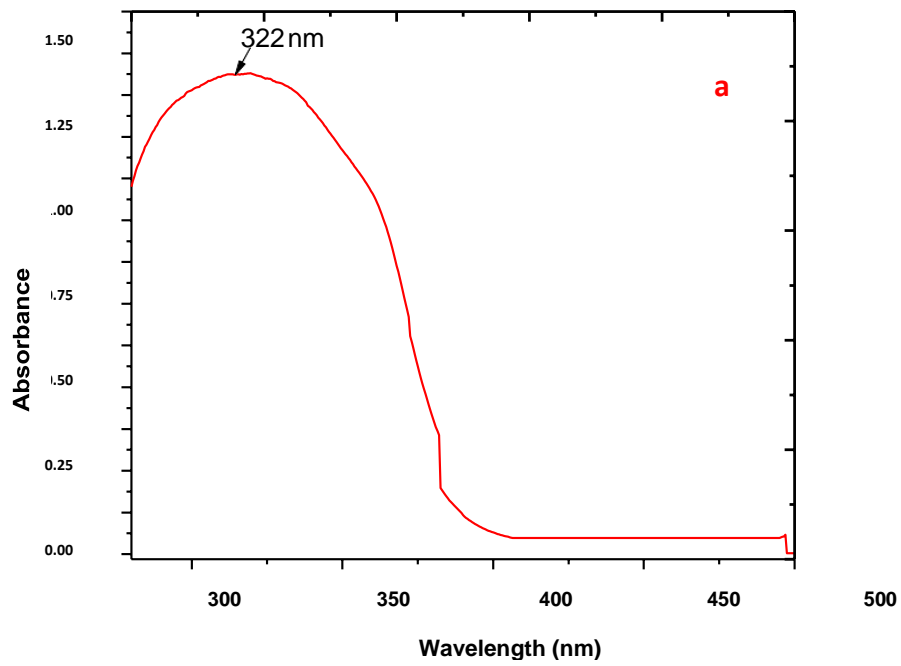


Figure 1. UV-VIS Analysis of Bulk (a) and Nano Zinc

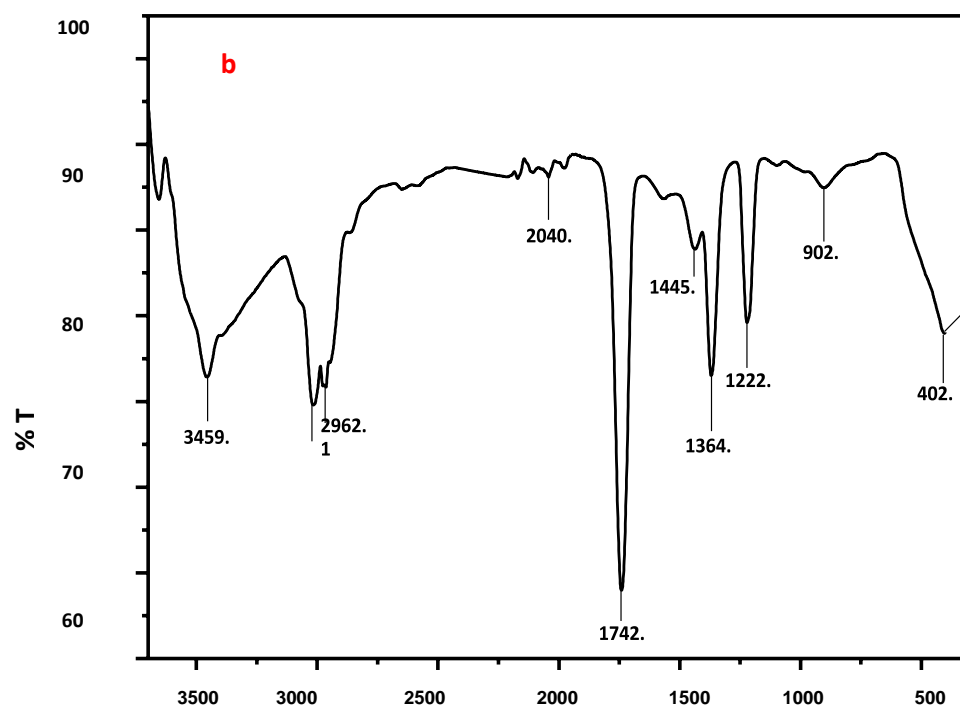
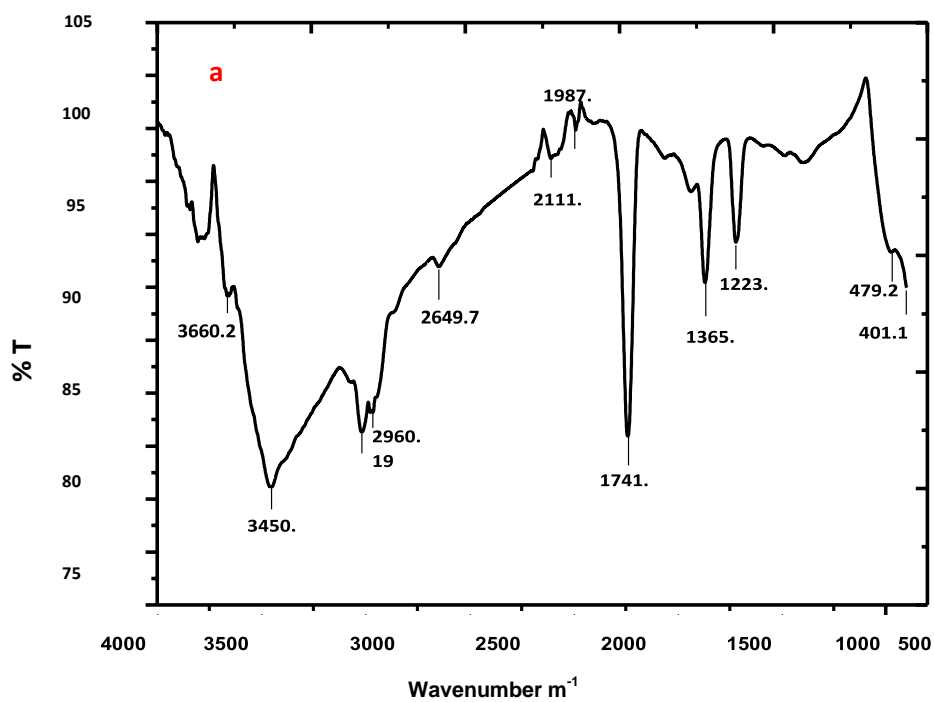


Figure 2. Fourier Transform Infrared Spectroscopy Analysis of Bulk(a) and Nano Zinc oxide(b)

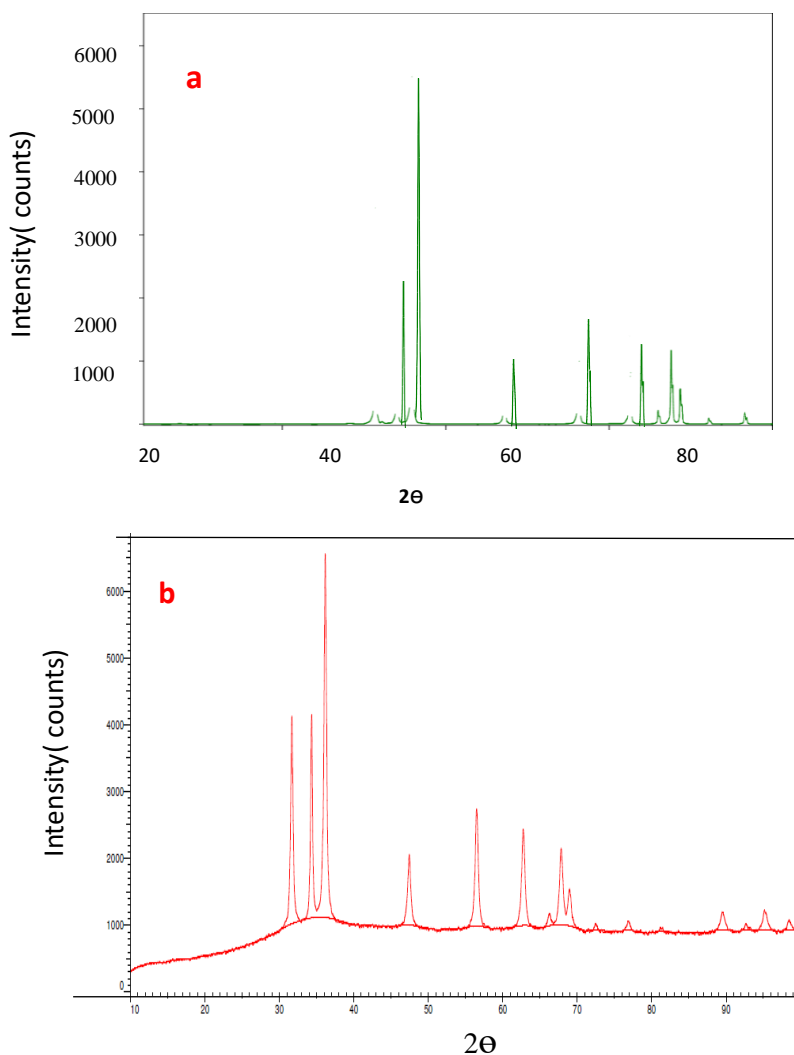


Figure 3. X-Ray Diffraction Analysis of Bulk(a) and Nano Zinc Oxide(b)

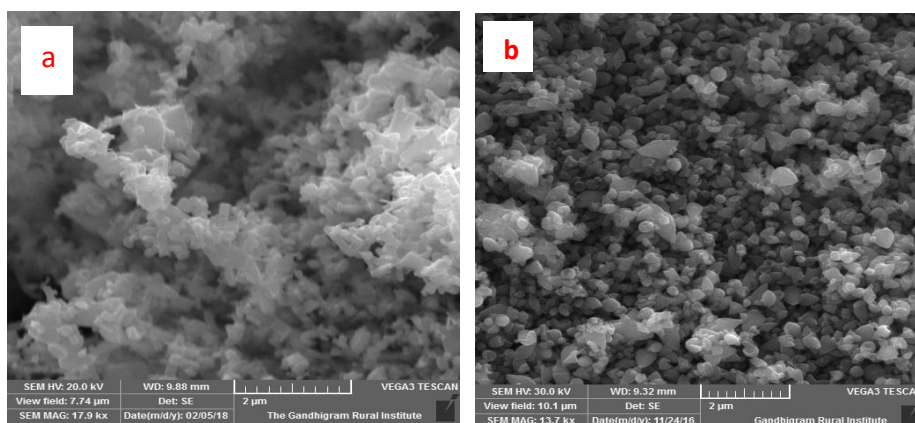


Figure 4. SEM Image of Bulk(a) and Nano Zinc Oxide(b)

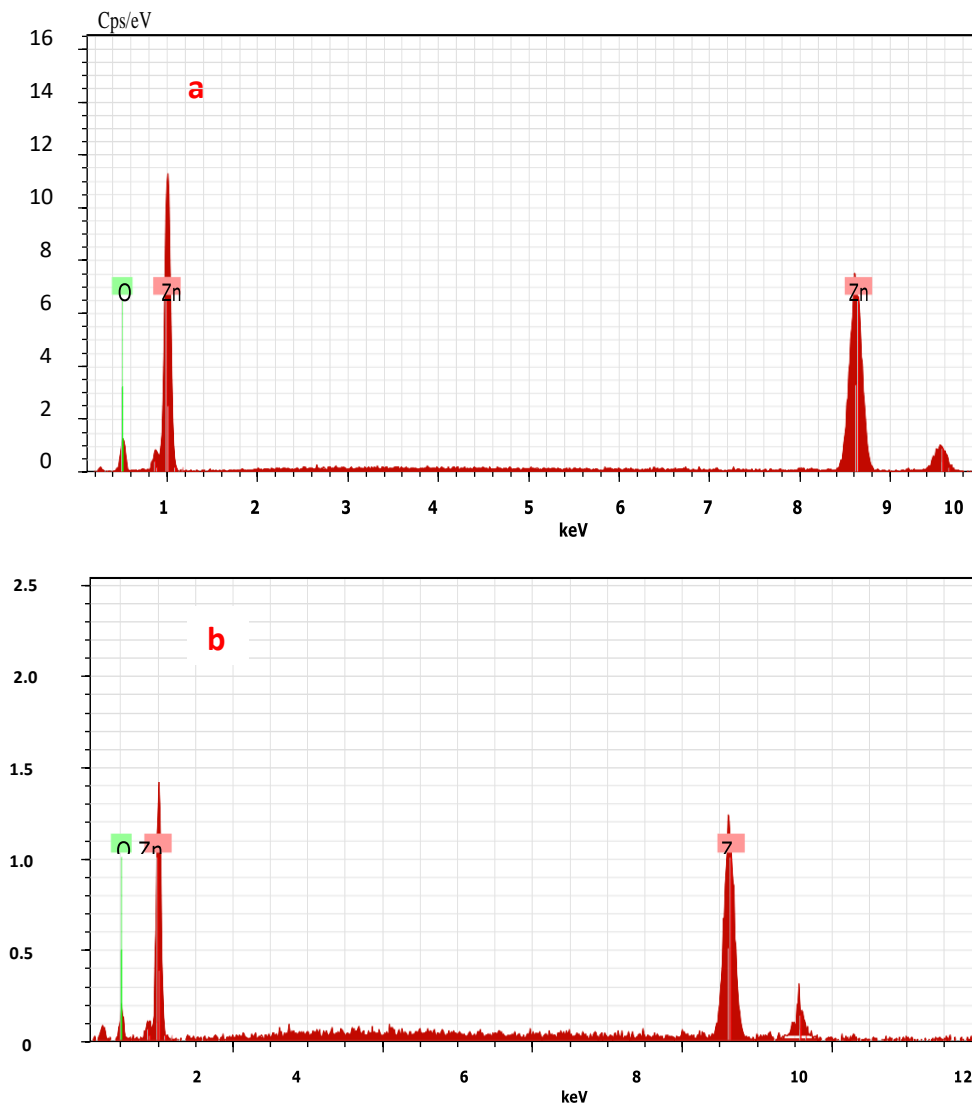


Figure 5. EDX Analysis of Bulk(a) and Nano Zinc Oxide(b)

Figures 8 and 9 illustrate various histological alterations in the liver of fish exposed to both bulk and nano zinc oxide at the end of the 7th and 14th day of treatment. Comparing the livers of the control and treatment groups, the liver in the control displays normal cell organisation (Figures 8 & 9 a, b). On the 7th and 14th day of the bulk treatment for liver tissue deterioration, more melanomacrophages, clogged portal vein or pancreatic tissue, and vacuolation with hepatic necrosis were seen. While in case of nano ZnO, treated fish liver (Figure 9 c to h) shows cytoplasmic vacuolation, apoptosis with condensed nuclear bodies, oedema, mononuclear cell infiltration, dilated sinusoids with shrinkages of pancreatic tissue and hepatic necrosis with decreased size of nuclei.

In contrast to treated fish that have been exposed to both bulk and nano ZnO, control fish have kidneys that display normal cell organisation. Figures 10 and 11 illustrate how kidney structure has changed from the 7th to the 14th day of exposure as the concentration of bulk and nanoparticles has increased. Bowman's capsule enlargement, tubular deformation, glomerular growth with constricting renal tubules, increased mononuclear cell infiltration, hemolysis, and hemosiderin with severe tissue degeneration are among the modifications.

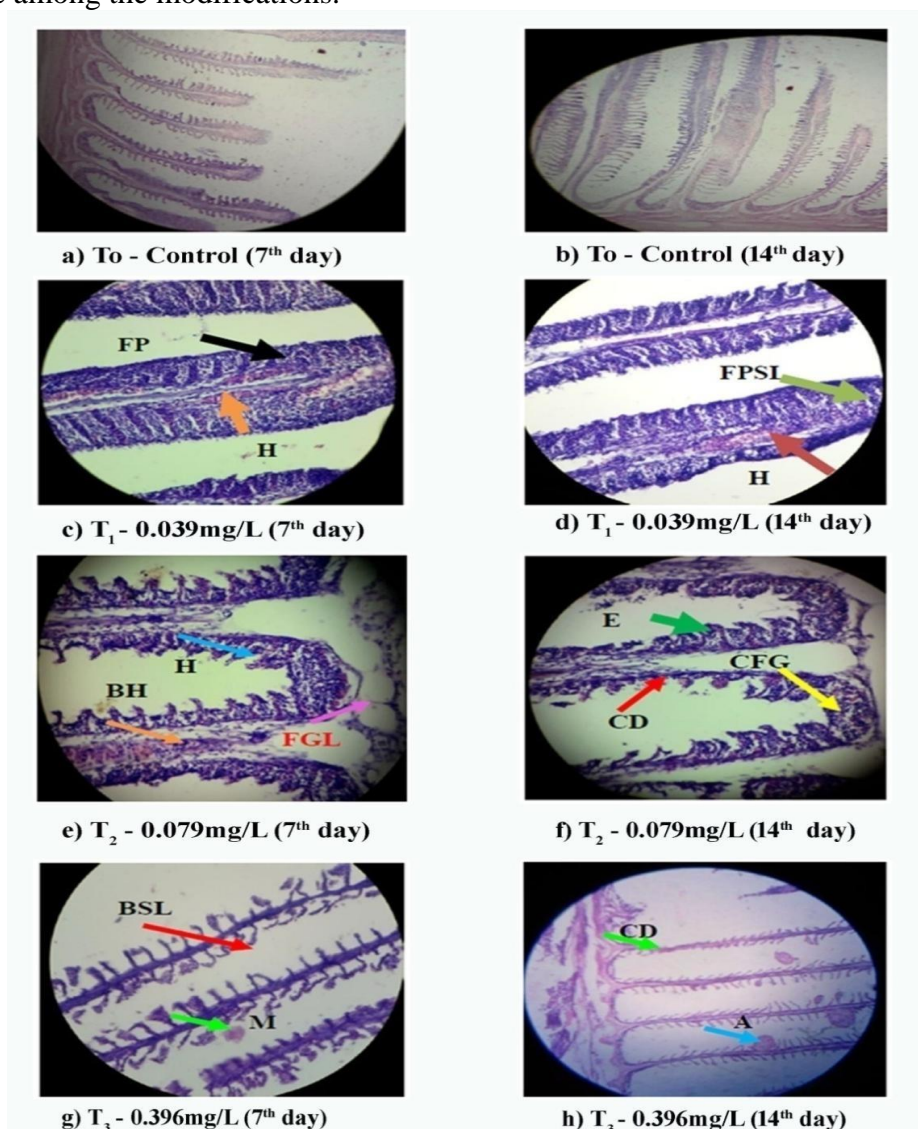


Figure 6. Histopathological changes in Gill of *Labeo rohita* exposed to Bulk Zinc Oxide

(FPSL- Fusion of Primary & Secondary Lamellae, H- Hemorrhages, BH-Basal Hyperplasia, FGL-Fusion of Gill Lamellae, E-Epithelial Fusion, CFG-Capillary Fusion of Gill Lamellae, BSL-Bending Secondary Lamellae, CD- Capillary Dilution, M- Mucus cell, A-Aneurysm)

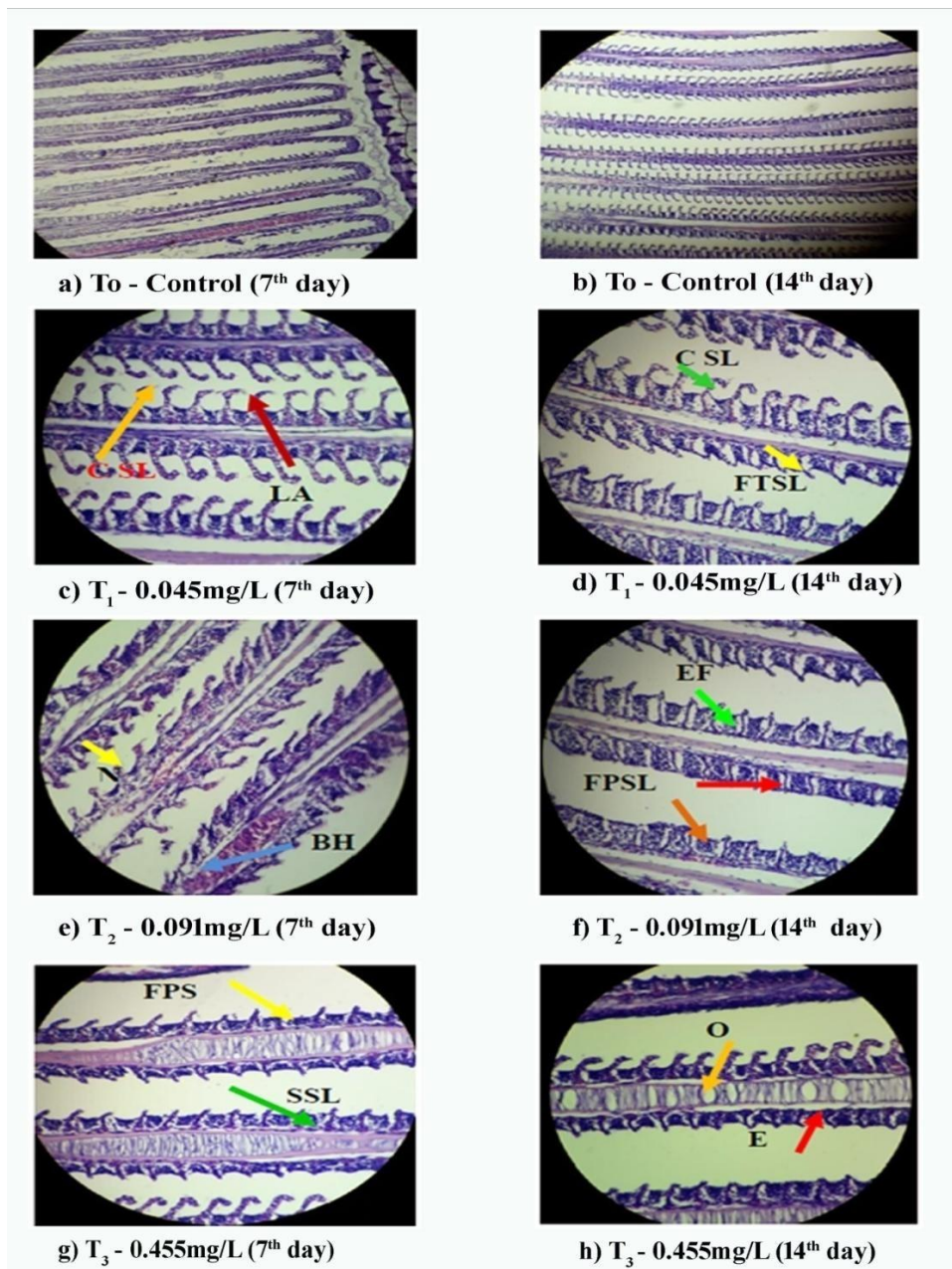


Figure 7. Histopathological changes in Gill of *Labeo rohita* exposed to Nano Zinc Oxide

CSL- Curling of Secondary Lamellae, LA- Lamellar Aneurysm, FTSL- Fusion at the tip of Secondary Lamellae, N- Necrosis, BH- Basal Hyperplasia, EF- Epithelial Fusion, FPSL- Fusion of Primary & Secondary Lamellae, SSL- Shortening Secondary Lamellae, O- Oedema

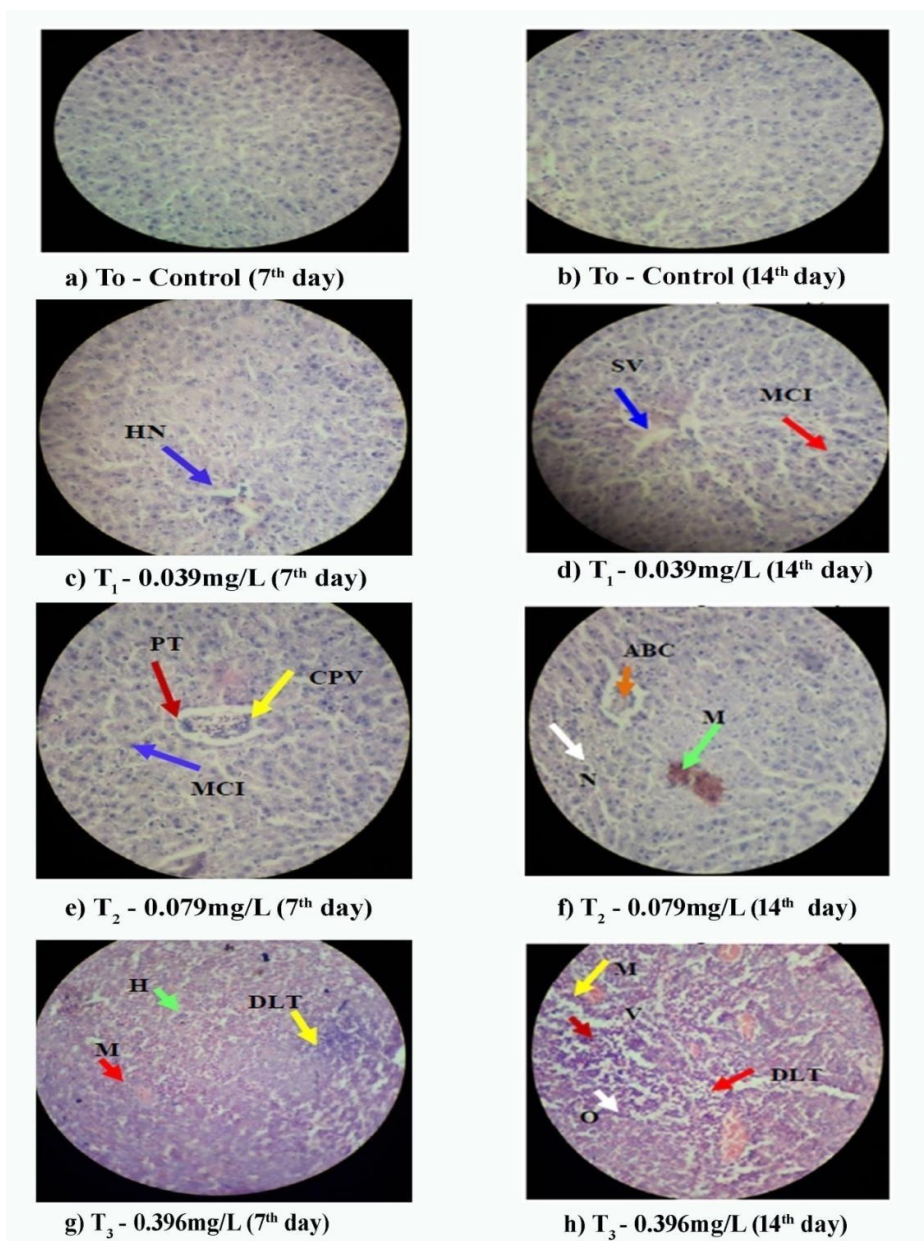


Figure 8. Histopathological changes in Liver of *Labeo rohita* exposed to Bulk Zinc Oxide

HN- Hepatic Necrosis, SV-Cytoplasmic Vacuolation, MCI-Mononuclear Cell Infiltration, PT-Pancreatic Tissue, CPV-Congested Portal Vein, N- Necrosis, ABC-Aggregated Blood Cell, M-Melanomacrophages, DLT-Degradation of Liver tissue, H- Hepatocytes, O-Oedema, MCI-Mononuclear Cell Infiltration, V-Vacuolation

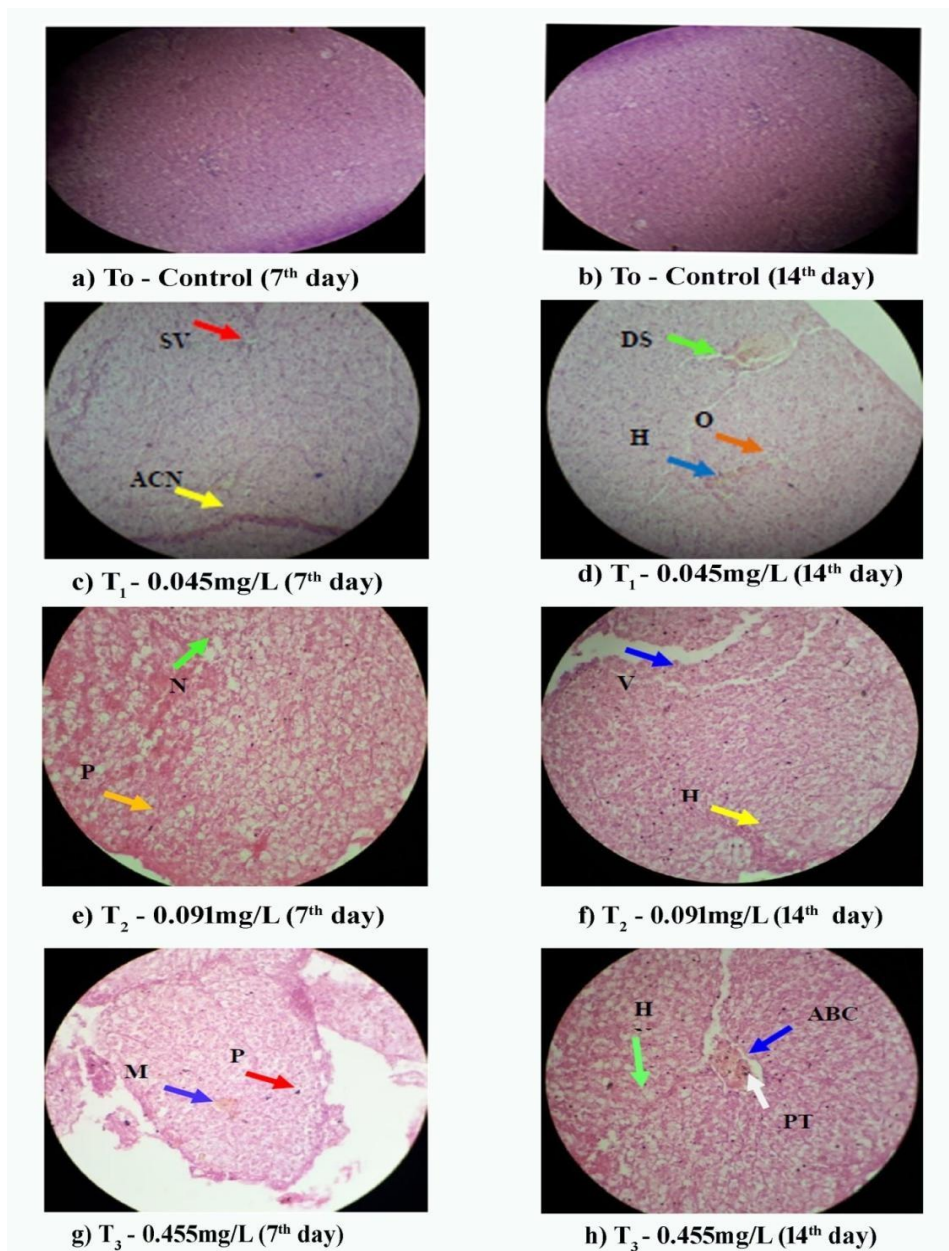


Figure 9. Histopathological changes in Liver of *Labeo rohita* exposed to Nano Zinc Oxide

SV- Cytoplasmic Vacuolation, ACN- Apoptosis with Condensed Nuclei, DS- Diluted Sinusoid, H- Hepatocytes, O-Oedema, N-Necrosis, P-Prokaryotic nuclei, V- Vacuolation, H- Hepatocytes, M- Melanomacrophages, ABC- Aggregated Blood Cell, PT- Pancreatic Tissue

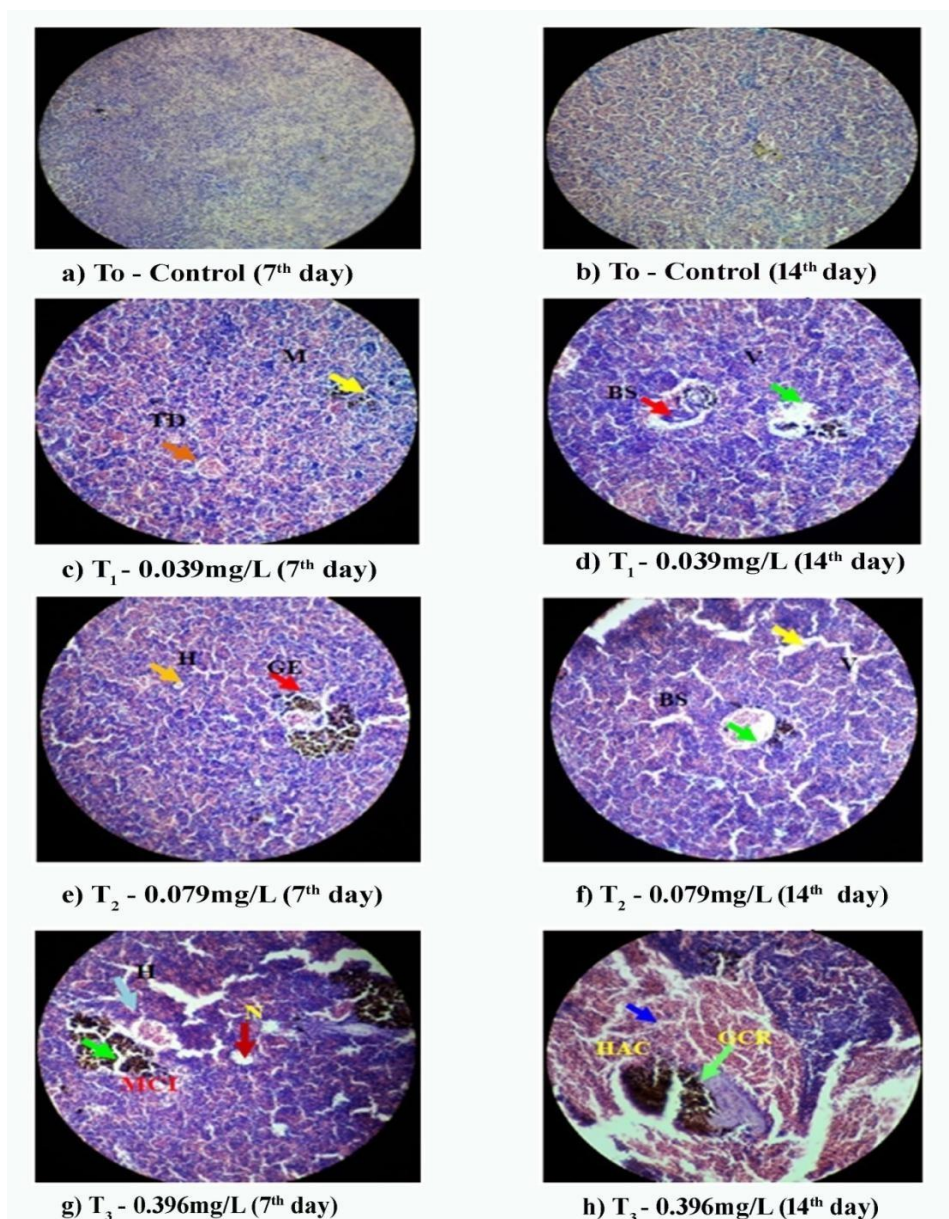


Figure 10. Histopathological changes in Kidney of *Labeo rohita* exposed to Bulk Zinc Oxide

TD-Tubular Deformation, M-Melanochyma cells, BS-Dilution of Bowman's Space, V-Vacuolation, BS- Dilation of Bowman's capsule Space, GE- Glomerular Expansion, H- Hemolysis, MCI- Mononuclear cell infiltration, N-Necrosis, GCR- Glomerular expansion with Constricted Renal tubule, HAC-Hemosiderin with Acute Cellular degeneration

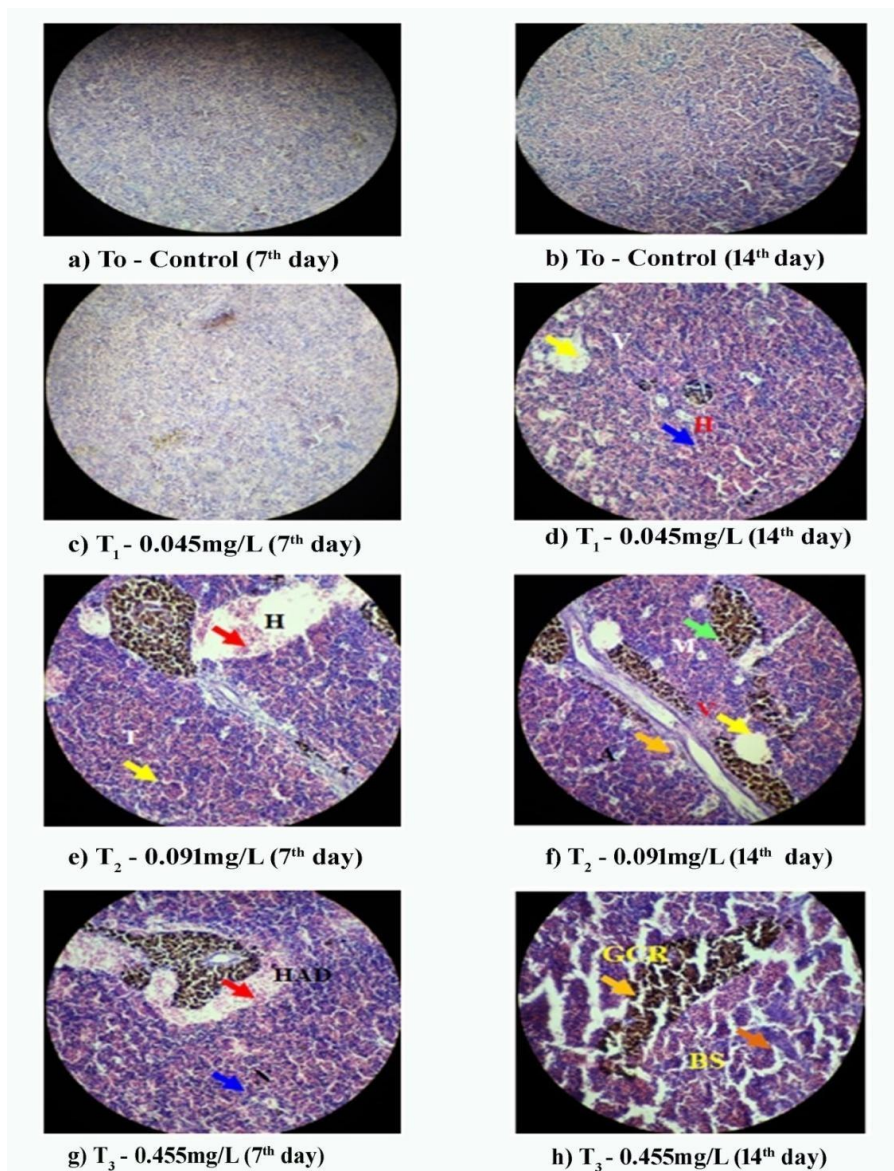


Figure 11. Histopathological changes in Kidney of *Labeo rohita* exposed to Nano Zinc Oxide

H- Hemolysis, V-Vacuolation, T- Tubular deformation, A-Apoptosis, M-Melanochyma cells, N-Necrosis, HAD-Hemosiderin with Acute Cellular degeneration, BS-Dilation of Bowman's capsule Space, GCR-Glomerular expansion with Constricted Renal tubule

Discussion

The main portrayal of bulk and chemically manufactured nano zinc oxide particles was interpreted by adopting UV-VIS Spectrophotometer and the vertex optical density was noticed at wavelengths 322nm and

335nm. Similar to this, Talam *et al.* (2012) observed a peak for nanoparticles of zinc oxide at 320 nm. Alwan *et al.* (2015) observed a single peak in absorbance at 345 nm, which suggests that ZnO nanoparticle size is nearly uniform. The functional group of bulk and nano ZnO was analyzed by Fourier transform infrared spectroscopy (FTIR) and peaks were observed. Similarly, Farag *et al.* (2010) found peaks at 3441 cm^{-1} due to vibrations stretching the O-H atom, 1636 cm^{-1} due to vibrations stretching the C=O atom of carboxylate anions absorbed into the outermost layer of ZnO particles, and 435 cm^{-1} due to vibrations stretching the Zn-O atom. The XRD diffraction peaks of bulk and nano ZnO particles are indexed at 31.687° (100), 36.172° (101), 47.453° (102), 56.507° (110), 62.768° (103), 76.908° (202), 98.472° (114) and at 31.371° (100), 47.161° (102), 56.223° (110), 62.492° (103), 72.210° (004), 78.833° (400) respectively with crystal plane (JCPDS card no. 36-1451) confirms that the particles were hexagonal wurtzite in structure and the calculated average crystalline size was 65nm and 24nm. The highly crystalline structure of ZnO was reported by Krol *et al.* (2017) and the purity of the sample is often assessed using the X-ray diffraction method. Bulk zinc oxide had a rod-like shape, whereas chemically synthesized nano zinc oxide had a spherical shape and a homogeneous distribution, as seen by SEM. Saptashi Ghosh *et al.* (2014) reported that SEM images of ZnO nanoparticles are sphere-shaped with a smooth exterior prepared by the chemical precipitation method. The purity of the particles is confirmed by the EDX spectrum, which was obtained for bulk and chemically generated ZnO and only contains Zn and O compound peaks. Just Zn and O peaks can be seen in the sample's EDX measurement, which verifies that the synthetic approach for making pure ZnO nanoparticles was successful (Goudarzi *et al.*, 2017).

Environmental toxins may cause pathological changes and changes in the histological structure of cells as a result of sub-lethal exposure. These changes may have a substantial impact on how fish tissues and organs function (Sultana *et al.*, 2016). According to Vinodhini and Narayanan (2009), histopathological studies have been widely utilised to explain the health condition of fish affected by pollution and serve as a gauge to measure the consequences of environmental pressure in fish and it also allows information about specific target organs or tissue that have been infected by aquatic pollution. In the present study, histological variation in the gill of *Labeo rohita* exposed to bulk and nano ZnO showed both types of injuries such as lamellar aneurysm, bending at the tip of secondary

lamellae, basal hyperplasia, necrotic lamellae, the proliferation of chloride cells, total fusion of primary and secondary lamellae, mucus cells, haemorrhage in primary lamellae and oedema at 7th and 14th-day exposure. Similarly, Alkaladi *et al.* (2014) and Hao *et al.* (2013) reported that the gill of *O. niloticus* exposed to ZnO NPs shows necrosis, epithelial cells with dilated mucous cells, oedema and mucus of chloride cell after the exposure period. Suganthi *et al.* (2015) and Subashkumar and Selvanayagam (2014) observed alterations in secondary lamellae, lamellar fusion, necrotic lamellae, the proliferation of chloride cells and mucus formation in gill epithelia of *C. Carpio* and *O. niloticus* respectively, treated with ZnO NPs after a period 14 days of exposure. Likewise, the gill of *O. niloticus* and *O. mossambicus* exposed to ZnO shows similar lesions such as basal hyperplasia and curling at the tip of secondary lamellae (Kaya *et al.*, 2016, Kaya *et al.*, 2017 Shahzad *et al.*, 2018).

In *Labeo rohita*, histopathology of the liver shows increased aggregation, melanomacrophages, a clogged portal vein, eosinophilic cytoplasm with hepatic necrosis, apoptosis with condensed nuclear bodies, oedema, mononuclear cell infiltration, dilated sinusoids with shrinkages of pancreatic tissue and decreased size of nuclei exposed to both bulk and nano ZnO at 7th and 14th-day exposure. Shahzad *et al.* (2018) reported that the liver of *O. mossambicus* exposed to ZnO nanoparticles shows necrosis and apoptosis with condensed nuclear bodies, pyknotic nuclei, and sinusoid spaces about parenchyma and oedema at the end of 14th day. In addition, Kaya *et al.* (2017) found that after 14th days of exposure to Zn NP suspensions at 10 mg/L, there was a rise in the number of hepatocytes and mononuclear cells infiltrating the liver of *O. niloticus*.

In the present study, fish in the control exhibit normal cell organisation in the kidney whereas, treated in both bulk and nano ZnO showed alternation such as dilation of Bowman's capsule, tubular deformation, glomerular expansion with constricted renal tubule, increasing of mononuclear cell infiltration, hemolysis and hemosiderin with severe cellular ageing. The kidney is the primary filtering organ in fish, capturing particles from the blood and maintaining renal filtration rates and osmoregulatory systems (Gupta *et al.*, 2016). Kaya *et al.*, (2016) reported significant melanomacrophages aggregation, glomerular expansion and deformation of renal tubule epithelium in *O. niloticus* treated with small and large ZnO nanoparticles at the end of 7th-day exposure paralleled to control. Hence, the present study concludes that bulk zinc oxide could be more toxic to the organs of *Labeo rohita* than that nano zinc oxide.

Acknowledgements

This research was supported by the Department of Biology, The Gandhigram Rural Institute- Deemed to be a University, Gandhigram, Tamil Nadu, India.

References

- Abdel-Warith, A. A., Younis, E. M., Al-Asgah, N. A. and Wahbi, O. M. (2011). Effect of zinc toxicity on liver histology of Nile tilapia, *Oreochromis niloticus*. Scientific Research Essays, 6:3760-3769.
- Agah, H., Leermakers, M., Elskens, M., Fatemi, S. M, and Baeyens, W. (2009). Accumulation of Trace metals in the muscle and liver tissues of five fish species from the Persian Gulf. Environmental Monitoring and Assessment, 157:499-514.
- Alkaladi, A., Afifi, M., Mosleh, Y. Y. and Zinada, O. A. (2014). Ultrastructure alteration of sublethal concentrations of zinc oxide nanoparticles on Nile tilapia (*Oreochromis niloticus*) and the protective effects of vitamins C and E. Life Science Journal, 11:257-262.
- Alwan, R. M., Kadhim, Q. A., Sahan, K. M., Ali R. A., Mahdi, R. J., Kassim, N. R. and Jassim, A. N. (2015). Synthesis of zinc oxide nanoparticles via sol gel route and their characterization. Nanoscience and Nanotechnology, 5:1-6.
- Can, E., Kizak, V., Kayim, M., Can, S. S., Kutlu, B., Ates, M., Kocabas, M. and Demirtas, N. (2011). Nanotechnological applications in aquaculture-seafood industries and adverse effects of nanoparticles on the environment. Journal of Materials Science Engineering, 5:605-609.
- Farag, H.K., Hanafi, Z.M., Dawy, M and Abd El Aziz, E.M (2010). Characterization of ZnO nanopowders synthesized by the direct precipitation method. Canadian Journal of Pure and Applied Science, 4:1303-1309.
- Goudarzi, M., Mousavi-Kamazani, M. and Salavati-Niasari, M. (2017). Zinc oxide nanoparticles: solvent-free synthesis, characterization and application as heterogeneous nanocatalyst for photodegradation of dye from the aqueous phase. Journal Material Science and Electronics, 28:8423-8428.
- Gupta, Y. R., Sellegounder, D., Kannan, M., Deepa, S., Senthilkumaran, B. and Basavaraju, Y. (2016). Effect of copper nanoparticles exposure in the physiology of the Common carp (*Cyprinus carpio*): Biochemical, histological and proteomic approaches. Aquaculture and Fisheries, 1:15-23.
- Hao, L., Chen, L., Hao, J. and Zhong N. (2013). Bioaccumulation and sub-acute toxicity of zinc Oxide nanoparticles in juvenile carp (*Cyprinus carpio*): a comparative study with its bulk counterparts. Ecotoxicology and Environmental Safety, 91:52- 60.
- Jeyabharathi, S., Kalishwaralal, K., Sundar, K. and Muthukumaran, A. (2017). Synthesis of zinc oxide nanoparticles (ZnO NPs) by aqueous extract of *Amaranthus caudatus* and evaluation of their toxicity and antimicrobial activity, Material Letters, 209:295-298.
- Jovanović, B. and Palić, D. (2012). Immunotoxicology of non-functionalized engineered nanoparticles in aquatic organisms with special emphasis on fish- review of current knowledge, gap identification, and call for further research. Aquatic Toxicology, 118:141-151.
- Kahru, A. and Dubourguier, H. C. (2010). From ecotoxicology to nanoecotoxicology. Toxicology, 269:105-119.
- Kaya, H., Aydın, F., Gürkan, M., Yılmaz, S., Ates, M., Demir, V. and Arslan, Z. (2016). A comparative toxicity study between small and large size zinc oxide nanoparticles in tilapia (*Oreochromis niloticus*): Organ pathologies, osmoregulatory responses and immunological parameters. Chemosphere, 144:571-582.
- Kaya, H., Duysak, M., Akbulut, M., Yılmaz, S., Gürkan, M., Arslan, Z., Demir, V. and

- Ateş, M. (2017). Effects of sub-chronic exposure to zinc nanoparticles on tissue accumulation, serum biochemistry and histopathological changes in tilapia (*Oreochromis niloticus*). *Environmental Toxicology*, 32:213-1225.
- Kaya, H., Duysak, M., Akbulut, M., Yılmaz, S., Gürkan, M., Arslan Z. and Ateş M. (2016). Effects of subchronic exposure to zinc nanoparticles on tissue accumulation, serum biochemistry, and histopathological changes in tilapia (*Oreochromis niloticus*). *Environmental Toxicology*, 32:1213-1225.
- Khan, I., Saeed, K. and Khan, I. (2019). Nanoparticles: Properties, applications and toxicities. *Arabian Journal of Chemistry*, 12:908-931
- Krol, A., Pomastowski, P., Rafinska, K., Railean Plugaru, V and Buszewski, B (2017). Zinc oxide nanoparticles: Synthesis, antiseptic activity and toxicity mechanism, *Advances in College Interface Science*, 249:37-52.
- Lennart Treuel, X. J. (2013). New views on cellular uptake and trafficking of manufactured nanoparticles. *Journal of the Royal Society, Interface / the Royal Society*, 449- 450.
- Murali, M., Suganthi, P., Athif, P., Sadiq Bukhari, A., Syed Mohamed, H. E., Basu, H. and Singhal, R. K. (2017). Histological alterations in the hepatic tissues of Al₂O₃ nanoparticles exposed freshwater fish *Oreochromis mossambicus*. *Journal of Trace Elements and Medical Biology*, 44:125-131.
- Nel, A., Xia, T., Madler, L. and Li, N. (2006). Toxic Potential of Materials at the Nanolevel. *Science*, 311:622-627.
- OECD (1992). Guidelines for the testing of chemicals. Fish, Acute Toxicity Test. Organization for Economic Cooperation and Development, Paris, France. 203.
- Riyadh, M. A., Quraish A. K., Kassim, M. S., Rawaa, A. A., Roaa, J. M., Noor, A. K. and Alwan, N. J. (2015). Synthesis of zinc oxide nanoparticles via sol – gel route and their characterization. *Nanosci. and Nanotech.*, 5: 1-6.
- Saptashi, G., Deblin, M. and Somenath, R. (2014). Facile sonochemical synthesis of zinc oxide nanoflakes at room temperature. *Material Letters*, 130: 215-217.
- Shahzad, K., Naeem Khan, M., Jabeen, F., Kosour, N., Shakoor Chaudhry, A., Sohail, M. and Ahmad, N. (2018). Toxicity of zinc oxide nanoparticles (ZnO NPs) in tilapia (*Oreochromis mossambicus*): tissue accumulation, oxidative stress, histopathology and genotoxicity. *International Journal of Environmental Science and Pollution*, 25:15943-15953.
- Subashkumar, S. and Selvanayagam, M. (2014). First report on Acute toxicity and gill histopathology of freshwater fish *Cyprinus carpio* exposed to Zinc oxide (ZnO) nanoparticles. *International Journal of Science Research Publication*, 4:1-4.
- Suganthi, P., Murali, M., Sadiq Bukhari, A., Syed Mohamed, H. E., Basu, H. and Singhal, R. K. (2015). Morphological and liver histological effects of ZnO nanoparticles on *Tilapia Mozambique*. *Journal of Advanced Applied Science and Research*, 1:68-83.
- Sultana, T., Butt, K., Sultana, S., Al-Ghanim, K. A., Mubashra, R., Bashir, N., Ahmed, Z., Ashraf, A. and Mahboob, S. (2016). Histopathological changes in liver, gills and intestine of *Labeo rohita* inhabiting industrial waste contaminated water of the river. *Pakistan Journal of Zoology*, 48:1171-1177.
- Talam, S., Karumuri, S. R. and Gunnam, N. (2012). Synthesis, Characterization and Spectroscopic Properties of ZnO Nanoparticles. *ISRN Nanotechnology*, 372505:1-6.
- Vinodhini, R. and Narayanan, M. (2009). Effect of heavy metals on the level of vitamin E, total lipid and glycogen reserves in the liver of common carp (*Cyprinus Carpio*). *Maejo International Journal of Science and Technology*, 2:391-399.

(Received: 29 June 2022, accepted: 30 December 2022)